Energy-Efficient Strategy for Improving Coverage and Rate Using Hybrid Vehicular Networks

Deepak Saluja, Rohit Singh, *Student Member, IEEE*, Nitin Saluja, and Suman Kumar

***Abstract*— A decade back, emergency voice communication was the only target to support the patient in an ambulance. It is now evolved from emergency voice communication to vital signal monitoring and operating the machines from the remote place. This evolution requires support from technology to meet the high data rates along with reliability for the specified applications. The millimeter-wave (mmWave) communication support high data rate requirements of vehicular communication. However, in the case of mmWave, the radio signals vary fast. It poses the implementation challenge to the mmWave system in this scenario. The other implementations challenges of mmWave are high path loss, severe blockage and frequent beam updates which inhibit seamless connectivity (reliability) to vehicular nodes. However, the reliability is always a prime concern for any vehicular communication system. This paper addresses these challenges by implementing a novel energy-efficient strategy based on RSUs deployment and radio access technology (RAT). The strategy is to deploy RSUs on either side of the road and use an optimal combination of mmWave and microwave RAT. The essential analysis of such a hybrid system involves the evaluation of parameters based on the analytic model. Hence, this paper analytically obtains the expression for seamless coverage and connectivity. The analysis is also extended to rate and energy efficiency calculations. The analysis is supported by probabilistic models-based simulations that agree closely with computation results. The results claim that the proposed model leads to improved performance in terms of coverage and rate while maintaining the cost and energy efficiency within the limits.**

***Index Terms*— Vehicular network, millimeter-wave communication, microwave communication, stochastic geometry, coverage probability, connectivity, energy efficiency.**

I. Introduction

IN RECENT years, vehicular communication via roadside-units (RSUs) (which includes vehicle-to-roadside (V2R) and roadside-to-vehicle (R2V) communication) has been widely used to support enhanced mobile broadband (eMBB) and ultra-reliable low-latency communication (URLLC) [1]–[3]. The emergency services, including safety application, fall under URLLC use case, seek reliability, and low-latency communication. On the other hand, services like multimedia communication, vital signal monitoring, and operating the machines from the remote place to support the patient in an ambulance, object detection and recognition, etc., fall under eMBB use case demand high data-rate [4], [5]. R2V communication uses the long-term evolution (LTE) connectivity in the Sub-6GHz band (microwave band), ensuring good reliability (coverage) [6], [7]. However, eMBB services prove to be challenging for the microwave network. A solution to this high data-rate demand can be found in millimeter-wave (mmWave) radio access technology (RAT) [8], [9]. However, mmWave is susceptible to high path-loss hence the coverage is limited to a shorter distance. Also, increasing RSU density reduces connectivity, because with the increase in RSU density, the probability that the vehicular node remains connected to its associated RSU for the complete duration of a fixed time slot decreases [10]. Further, the connectivity also depends on the main lobe beam-width of an antenna at RSU. It is concluded from the discussion that there are considerable challenges with mmWave R2V communication.

Considering these challenges of mmWave communication, a feasible solution is to integrate it with microwave communication. This paper proposes a hybrid of mmWave and microwave networks. The aim of this study is to offer a method to achieve high data-rate (to support specified applications) along with reliability while maintaining the cost and energy efficiency within the limits.

A. Related Work

The integration of mmWave and microwave communications requires a detailed analysis of both technologies in the vehicular communication environment. A large number of papers are available in the literature that offers detailed studies of both technologies. The analysis of V2R/R2V communication involving microwave connectivity is presented in [6], [7], [11]–[13], while a similar analysis involving mmWave connectivity is performed in [10], [14]–[19]. The different methodologies are presented in [14], [15] to optimize resource utilization in R2V communication. For instance, the placement of RSUs in highways with multiple lanes are optimized in [14]. The algorithm for complexity reduction is presented in [15]. The performance of the downlink R2V networks in terms of coverage, rate, and energy efficiency has been investigated in [6], [10], [16]–[19]. The article [6] considered the dynamic resource allocation for minimizing power consumption. The performance improvement in terms of energy efficiency and delay has been offered in [16] using the femto access points.

Manuscript received January 12, 2020; revised June 1, 2020; accepted July 20, 2020. The Associate Editor for this article was H. Dong. *(Corresponding author: Deepak Saluja.)*

Deepak Saluja, Rohit Singh, and Suman Kumar are with the Department of Electrical Engineering, IIT Ropar, Ropar 140001, India (e-mail: 2016eez0009@iitrpr.ac.in; 2017eez0007@iitrpr.ac.in; suman@iitrpr.ac.in).

Nitin Saluja is with the Chitkara University Institute of Engineering and Technology, Chitkara University, Rajpura 140401, India (e-mail: nitin.saluja@chitkara.edu.in).

Digital Object Identifier 10.1109/TITS.2020.3011890

The coverage performance for the mmWave network has been investigated in [17]. In [18], the authors have developed an analytical framework to obtain the throughput under cooperative communication. The issues of high data rate in the microwave networks are addressed in [10], [19] by employing the mmWave network. However, these works pose a significant challenge in ensuring the reliability of the vehicular system, especially in non line-of-sight (NLoS) scenario.

In [20], the authors emphasized on the content-sharing problem in cellular D2D networks. While, in [21], the authors proposed an algorithm to address the dependable content-sharing issue in Device-to-Device (D2D) cooperative vehicular networks, by employing big-data based vehicle trajectory prediction along with coalition formation game based resource allocation. Some existing works revealed that RSUs can also be used as fog nodes [22], [23]. They can perform data computations and afford data storage facilities. In [24], the authors analyzed the coverage and rate performance of a downlink cellular vehicle-to-everything communication network. While some authors have focused on eMBB and URRLC scenarios in 5G to improve the data transmission rate and reliability in the vehicular network [25]–[27]. In particular, the authors in [25] evaluated the performance of the downlink R2V networks in terms of reliability and latency for 5G autonomous vehicular networks. Whereas, the authors in [26] proposed a resource allocation scheme to enhance the video quality of eMBB services in vehicular networks. The joint scheduling of eMBB and URLLC traffic in the vehicular network is considered in [27]. Recently, the authors in [28] considered the radio resource allocation problem in the downlink of an R2V networks for URLLC vehicular networks.

It is evident from the literature that the work is progressed in the direction of a trade-off between coverage and rate. However, it is possible to achieve both the coverage and rate if the algorithm is defined to interface mmWave and microwave communication in a hybrid manner. This paper addresses this research gap exploiting advantages for both the technologies. The research on cellular networks operating in hybrid mmWave and microwave communication has been pretty widespread (e.g., [29]–[33]). However, there is a very limited work which considers the vehicular network involving both mmWave and microwave networks (e.g., [34], [35]). In [34], Hu *et al.* proposed a cluster-based algorithm for vehicular communication which involves hybrid of mmWave and microwave. In this algorithm, vehicles are divided into clusters, and each cluster has a cluster head (CH), primary nodes (vehicles in LOS with CH) and secondary nodes (all other vehicles). The RSUs communicate with vehicles using the microwave link, while vehicles communicate with each other using the mmWave link. The work is not efficient from the stability point of view. Hence, in [35], Zhang *et al.* extended the same work by introducing the cluster-based broadcast scheduling scheme to maintain the stability of CH. However, these works [34], [35] suffer from several problems, from both CH and secondary nodes perspective. From the CH perspective, it can suffer from heavy load while serving many primary nodes. Moreover, CH cannot enjoy a high data rate since it relies on the microwave band for its operation. From the secondary node perspective, there may exist NLoS path; consequently, there is a high probability that the mmWave interface will not work. This paper proposes a hybrid of mmWave and microwave vehicular network in R2V communication environment (see Fig. 1).

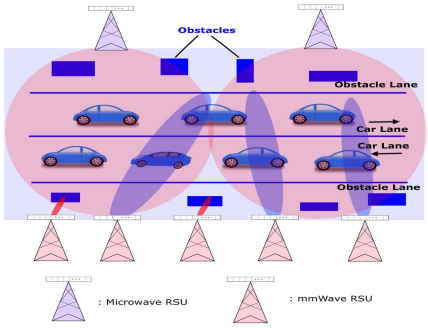

Fig. 1. Hybrid vehicular network scenario.

B. Contributions and Outcomes

The scope of the paper is to combine the merits of mmWave and microwave communication to improve the performance of vehicular network in R2V communication environment. The aim is to achieve high rate (to support multimedia applications) along with reliability while maintaining the cost and energy efficiency within the limits. The key contributions of this paper can be listed as follows:

- Unlike the existing work on the vehicular network, which considered either the mmWave vehicular network[1] or the microwave vehicular network,[2] we modeled/proposed a hybrid vehicular network, where both the mmWave and microwave RSUs are used in a hybrid manner. The number of microwave RSUs deployed in the proposed network is decided based on the maximum coverage probability corresponding to the microwave network. We used the stochastic-geometry to evaluate the performance of the proposed network. In addition, we introduce an association strategy for the proposed networks, that ensures a high rate along with a good coverage probability for the vehicular node.
- The expressions of coverage probability and connectivity are obtained for the proposed network. Further, the proposed network is compared with the mmWave vehicular network. It is shown that the proposed network outperforms the mmWave vehicular network in terms of coverage probability and connectivity. The numerical outcomes are validated with Monte Carlo simulations.
- The analysis is extended to average rate and energy efficiency calculations for the proposed network and compared with the mmWave vehicular network. It is shown that the proposed network improves the average rate and energy efficiency in comparison to the mmWave vehicular network.
- The impact of various parameters on network performance has been analyzed to draw some useful insights

[1] In mmWave vehicular network, only mmWave RSUs are used.
[2] In microwave vehicular network, only microwave RSUs are used.

TABLE I
SUMMARY OF NOTATIONS

Notation	Description
$r, \hat{r}$	Distance of reference vehicular node from its serving mmWave and microwave RSU, respectively
ξ_m	Set of mmWave RSUs modeled by 1-D PPP
ξ_μ	Set of microwave RSUs modeled by 1-D PPP
λ_m, λ_μ	Density of mmWave RSUs, microwave RSUs
λ_T	Density of mmWave + microwave RSUs
f_m, f_μ	mmWave carrier frequency, microwave carrier frequency
P_t	Transmit power of mmWave or microwave RSU
Q	Characterize the radio access technology (RAT) (i.e., either mmWave (m) RAT or microwave (μ) RAT)
c_0	Near field path loss at 1 m distance, $c_0 = \left(\frac{\lambda_Q}{4\pi}\right)^2$
ψ_M, G_S, g_S	Beamwidth of main lobe, main lobe gain, side lobe gain of directional antenna pattern for mmWave RSU
G_I	Antenna gain of mmWave interfering link
T_S, V	Slot duration, vehicle speed
$\Upsilon_T, \Upsilon_{th}$	Target SINR, SINR threshold
$2W, w, L$	Total road width, lane width, road length
h_O, H_U, λ_O	Height of obstacles (in meters), height of RSU (in meters), obstacle density
σ_m^2, σ_μ^2	Noise power added by mmWave and microwave RSU
$\{L, NL\}$	Possible types of links: L denotes LOS link, NL denotes NLOS link
$\alpha_{m,L}; \alpha_{m,NL}$	Path loss exponent for LOS and NLOS link in mmWave RAT, respectively
$\alpha_{\mu,L}; \alpha_{\mu,NL}$	Path loss exponent for LOS and NLOS link in microwave RAT, respectively
$\mathcal{P}_{mL}, \mathcal{P}_{\mu L}$	LOS probability for mmWave and microwave link respectively
Υ_m, Υ_μ	SINR of reference vehicular node associated with mmWave and microwave RSU, respectively
P_c, P_{ADC}	Circuit power consumption, power consumption due to analog-to-digital converter (ADC)

into network design. It has been shown that the hybrid network requires lesser number of RSUs in comparison to mmWave RSUs. Further, it is shown that difference in connectivity probability between hybrid and mmWave networks is significant at a lower density of mmWave RSUs. However, at a higher density of mmWave RSUs, the microwave RSUs in the hybrid network acts as a backup link to mmWave RSUs.

The summary of notations listed in Table I are used throughout the paper.

II. SYSTEM MODEL

A. Network Model

We modeled a downlink R2V vehicular network consisting of vehicular nodes and RSUs, which are deployed over a road of length L and width $2W$, as shown in Fig. 2. We assumed that the total road width is divided into 4 parts, resulting in

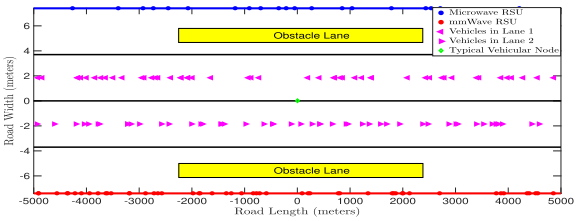

Fig. 2. Illustration of proposed network model.

a 4 parallel lanes, each having a width of $w = W/2$. The innermost lanes (i.e., Lane 1 and Lane 2) of the road are used by small and fast-moving vehicles, while the outermost lanes of the road are reserved for large and slow-moving vehicles, which acts as an obstacle for the vehicles in the innermost lane of the road. We have designated this lane as an obstacle lane. Note that the analysis is carried out for the reference vehicular nodes[3] lie in the innermost lane. Moreover, we assume that the reference vehicular node is located at the center of the road.

The modeled network uses both the mmWave and microwave RSUs in hybrid manner, where the mmWave RSUs are distributed according to a poison point process (PPP) ξ_m with density λ_m on one side of the road, while the microwave RSUs are distributed according to another independent poison point process (PPP) ξ_μ with density λ_μ on the other side of the road. We assume that obstacles of fixed height H_O, are randomly placed in the obstacle lane. If the straight line between the RSU and the reference vehicular node does not cross any obstacles, then the transmission occurs in LoS propagation conditions; otherwise, the transmission occurs in NLoS propagation conditions.

B. Channel Model

The transmission of a signal via the wireless channel is modeled by small-scale fading and path-loss attenuation. Here, we consider a Rayleigh fading[4] and standard power-law path loss model [37]. We consider two states of a link between the reference vehicular node and the serving RSU i.e., either LoS or NLoS, and correspondingly defines the path loss functions. The path loss function corresponds to the state of link S separated by a distance r is defined as [38]: $PL_{Q,S}(r) = c_0(r^2 + H_U^2)^{-\frac{\alpha_{Q,S}}{2}}$, where, $c_0 = (\frac{\lambda_R}{4\pi})^2$ denotes the path loss at 1 m distance. H_U denotes the height of RSU. Here, the notation R in the subscript distinguish the type of RAT i.e., either mmWave (m) RAT or microwave (μ) RAT used by RSU, while $\alpha_{Q,S}$ denotes the path-loss exponents corresponds to state of link S and RAT Q. The state of a link depends on several factors i.e., the distance between the reference vehicular node and serving RSU (r), the height of obstacles (H_O), the height of RSU (H_U), and type of

[3]reference vehicular node is the one for which the complete analysis is carried out.

[4]It can be seen from the existing literature ([10], [36]) that considering a general fading model (i.e., Nakagami-m fading) does not provide any additional useful insights in comparison to Rayleigh fading, while it complicates the analysis considerably. Hence, in this work we consider Rayleigh fading, and leave extensions to more general fading models as future work.

RAT (Q) used by RSU. These links can be characterized by its probabilistic behavior. We consider a distance-dependent probability function for microwave RAT. A commonly used distance-dependent LoS/NLoS propagation model is the 3GPP LoS/NLoS model [39], which is characterized by its LoS probability function $\mathcal{P}_{\mu,L}(r) = \min(\frac{18}{r}, 1)(1 - e^{-\frac{r}{36}}) + e^{-\frac{r}{36}}$.

In contrast, for mmWave, we consider a practical probabilistic model, that considers the link distance, the RSU height, and blockage density [38]. We denote the blockage density that defines the number of obstacles in the one-meter distance by λ_O. The probability of LoS link for mmWave is given by $\mathcal{P}_{m,L}(r, \Xi) = e^{-\lambda_O \Xi r}$, where the parameter $\Xi = \min(\frac{h_O}{H_U}, 1)$.

The actual path loss for mmWave RSU (denoted by $L(r)$) and microwave RSU (denoted by $\hat{L}(r)$) that consider the impact of LoS and NLoS model is given as:

$$L(r) = L_{m,L}(r)\mathcal{P}_{m,L}(r, \Xi) + L_{m,NL}(r)(1 - \mathcal{P}_{m,L}(r, \Xi)) \quad (1)$$

$$\hat{L}(r) = L_{\mu,L}(r)\mathcal{P}_{\mu,L}(r) + L_{\mu,NL}(r)(1 - \mathcal{P}_{\mu,L}(r)) \quad (2)$$

C. SINR Calculation

The channel fading gain between the reference vehicular node and mmWave RSU or microwave RSU is considered to be Rayleigh distributed with unit mean, thereby the corresponding channel power gain is exponentially distributed (i.e., $\sim$ exp(1)). Both the mmWave and microwave RSUs are assumed to transmit at a fixed power of P_t. The noise power corresponds to mmWave RSU and microwave RSU are denoted by σ_m^2 and σ_μ^2, respectively. The SINR Υ_m of a reference vehicular node associated with mmWave RSU, at a distance r meter is given by

$$\Upsilon_m = \frac{P_t g_1 G_S L_1(r)}{\sigma_m^2 + I_m}, I_m = \sum_{j \in \xi_m} P_t g_j G_I L_j(r), \quad (3)$$

where, g_1, and g_j denote the channel fading power from the reference vehicular node to serving mmWave RSU, and interfering mmWave RSUs, respectively. While $L_1(r)$, and $L_j(r)$ denote their corresponding path loss functions that can be obtained from (1). Note that G_S and G_I denote the gain of the main lobe, and the gain of interfering link, respectively for mmWave network. The SINR Υ_μ of a reference vehicular node associated with microwave RSU, at a distance $\hat{r}$ meter is given by

$$\Upsilon_\mu = \frac{P_t \hat{g}_1 \hat{L}_1(\hat{r})}{\sigma_\mu^2 + I_\mu}, I_\mu = \sum_{j \in \xi_\mu} P_t \hat{g}_j \hat{L}_j(\hat{r}), \quad (4)$$

where, $\hat{g}_1$, and $\hat{g}_j$ denote the channel fading power from the reference vehicular node to serving microwave RSU, and interfering microwave RSUs, respectively. While $\hat{L}_1(r)$, and $\hat{L}_j(r)$ denote their corresponding path loss functions that can be obtained from (1).

D. Modeling of Beamforming

The actual beamforming model for mmWave RSU is approximated by a sectored antenna model, which considers the main lobe beam-width (ψ_M), main lobe gain (G_S), and the side lobe gain (g_S) of an antenna pattern. The effective antenna gain pattern of a serving mmWave RSU towards reference vehicular node is formulated as a function of angle ψ from the boresight direction, which is given as

$$G_B(\psi) = \begin{cases} G_S, & \text{if } |\psi| \leq \frac{\psi_M}{2}. \\ g_S, & \text{otherwise.} \end{cases} \quad (5)$$

Moreover, the interfering links forms beam towards other vehicles which are modeled as a uniformly random variable in $[-\pi, \pi]$. Therefore, the effective antenna gain of an interfering link (G_I) is G_S with a probability of $P_S = \frac{\psi_M}{2\pi}$, and is g_S with a probability of $p_S = 1 - \frac{\psi_M}{2\pi}$.

III. RSU Deployment Strategy and Coverage Analysis

In this section, we formulate the strategy for deploying the mmWave and microwave RSUs along the road for the hybrid vehicular network, and obtain the coverage probability expression. We first deploy the microwave RSUs along one side of the road. The number of microwave RSUs deployed in a hybrid network is based on the optimal RSUs density of microwave vehicular network. The optimal RSUs density is corresponding to the RSUs density for which the coverage probability of microwave network is maximum. At optimal RSU density, signal power dominates the interference power. However, with further increase in density, interference power starts dominating the signal power. Further, we deploy the mmWave RSUs on another side of the road. The performance of the hybrid vehicular network is analyzed under the optimal density of microwave RSUs.

We assume that the vehicular node would associate either to the nearest mmWave RAT or to the nearest microwave RAT. The probability density function (pdf) of the distance from reference vehicular node to the nearest mmWave RSU is given by [10] i.e.,

$$f_M(r) = \frac{2\lambda_m r}{b(r)} e^{-2\lambda_m b(r)}, \quad (6)$$

while the pdf of the distance from reference vehicular node to the nearest microwave RSU is given by [10] i.e.,

$$f_\mu(\hat{r}) = \frac{2\lambda_\mu \hat{r}}{b(\hat{r})} e^{-2\lambda_\mu b(\hat{r})}, \quad (7)$$

where $b(i) = \sqrt{i^2 - W^2}$, $i \in \{r, \hat{r}\}$. First, we obtain the coverage probability expressions for microwave vehicular networks.

Lemma 1: The average coverage probability expression for a reference vehicular node served by microwave RSU, and at a distance of $\hat{r}$ meter from the associated microwave RSU is given by

$$P_{cov,\mu} = \int_W^\infty \left[exp\left\{ \frac{-\Upsilon_T {\sigma_\mu}^2}{P_t \hat{L}_1(\hat{r})} \right\} exp\{-2\lambda_\mu F(\hat{r}, \Upsilon_T)\} \right] \times f_\mu(\hat{r}) d\hat{r}. \quad (8)$$

where, $F(\hat{r}, \Upsilon_T) = \int_{\hat{r}}^\infty \frac{\Upsilon_T \hat{L}_j(x)}{\hat{L}_1(\hat{r}) + \Upsilon_T \hat{L}_j(x)} dx$, and $f_\mu(\hat{r})d\hat{r}$ is given by (7).

Proof: See Appendix A for the proof. ■

It is important to note that the coverage due to microwave RSUs peaks at a certain value of λ_μ. We are interested in

finding such a value ($\lambda_{\mu,opt}$), which can be easily obtained by setting the partial derivative of CP_μ about λ_μ to zero, i.e.,

$$\lambda_{\mu,opt} = \arg\limits_{\lambda_\mu} \left\{ \frac{\partial CP_\mu(\lambda_\mu, \Upsilon_T)}{\partial \lambda_\mu} = 0 \right\} \tag{9}$$

The coverage probability corresponds to optimal value of microwave RSUs density $\lambda_{\mu,opt}$ can be expressed as

$$P_{cov,\mu,opt} = \int_W^\infty \exp\left\{ -\frac{\Upsilon_T {\sigma_\mu}^2}{P_t \hat{L}_1(\hat{r})} \right\} \exp\{-2\lambda_{\mu,opt} F(\hat{r}, \Upsilon_T)\} \times f_\mu^*(\hat{r}) d\hat{r} \tag{10}$$

$$\text{where,} \quad f_\mu^*(\hat{r}) = \frac{2\lambda_{\mu,opt}\hat{r}}{b(r)} \exp\{-2\lambda_{\mu,opt} b(\hat{r})\}. \tag{11}$$

Next, we obtain the coverage probability expressions for the mmWave vehicular networks.

Lemma 2: The average coverage probability expression for a reference vehicular node served by mmWave RSUs, and at a distance of r meter from the associated mmWave RSU is given by

$$P_{cov,m} = \int_W^\infty \left(exp\left\{ \frac{-\Upsilon_T {\sigma_m}^2}{P_t G_M L_1(r)} \right\} exp\{-2\lambda_m G(r, \Upsilon_T)\} \right) \times f_M(r) dr. \tag{12}$$

where $G(r, \Upsilon_T) = \int_r^\infty \frac{\Upsilon_T G_I L_j(x)}{G_M L_1(r) + \Upsilon_T G_I L_j(x)} dx$, *and* $f_M(r)$ *is given by* (6).

Proof: See Appendix B for the proof. ∎

A. Coverage Probability of Hybrid Vehicular Network

A hybrid vehicular network considers both the mmWave and microwave RSUs, where reference vehicular node would connect to either nearest mmWave RSU or nearest microwave RSU based on predefined SINR threshold. If received SINR of mmWave RSU is greater than the predefined SINR threshold, the reference vehicular node would connect to mmWave RSU. Otherwise, it would connect to microwave RSU. Now, we obtain the coverage probability of the hybrid vehicular network which involves the calculation of coverage probability provide by both the mmWave RSU and microwave RSU.

Theorem 1: The average coverage probability provided by mmWave RSUs in hybrid mmWave and microwave vehicular network scenario is given by

$$P_{cov,m,PS} = \int_W^\infty exp\left\{ \frac{-max(\Upsilon_T, \Upsilon_{th}) {\sigma_m}^2}{P_t G_M L_1(r)} \right\} \times exp\{-2\lambda_m H(r, \Upsilon_T, \Upsilon_{th})\} f_M(r) dr, \tag{13}$$

where, $H(r, \Upsilon_T, \Upsilon_{th}) = \int_r^\infty \frac{max(\Upsilon_T, \Upsilon_{th}) G_I L_j(x)}{G_M L_1(r) + max(\Upsilon_T, \Upsilon_{th}) G_I L_j(x)} dx$, *and* $f_M(r)$ *is given by* (6).

Proof: See Appendix C for the proof. ∎

Theorem 2: The average coverage probability provided by microwave RSUs in hybrid vehicular network is given by (14)*, as shown at the bottom of the next page, where* $F(\hat{r}, \Upsilon_T)$ *and* $G(r, \Upsilon_{th})$ *are defined in Lemma 1 and Lemma 2, respectively, while* $f_M(r)$ *and* $f_\mu^*(\hat{r})$ *are given by* (7) *and* (11)*, respectively.*

Proof: See Appendix D for the proof. ∎

The effective coverage probability of hybrid vehicular network can be obtained by adding (13) and (14).

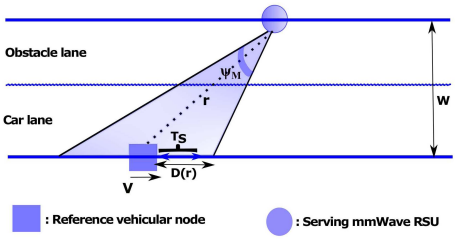

Fig. 3. Illustration of an half section of considered vehicular network. Where, $D(r)$ defines the maximum distance that the vehicular node can cover before leaving the communication range of its serving RSU. At the beginning of T_S, the serving RSU is connected and aligned towards reference vehicular node.

IV. Connectivity Analysis

We assume that the beam direction of RSU is updated only at the beginning of the time slot (T_S).[5] Initially, the RSU points its main lobe beam towards the reference vehicular node at the beginning of every T_S, as illustrated in Fig. 3. Let the reference vehicular node is connected to a particular RSU (let's say R^*) at the beginning of time slot with probability P_{cov}. Connectivity probability defines the probability with which the vehicular node remains connected to its associated RSU R^* for the complete duration of considered time slot [10], and is given by

$$P_{conn} = P_{cov} P_{RC}, \tag{15}$$

where, P_{RC} models the conditional probability with which the vehicular node remains connected to its associated RSU R^* for the complete duration of considered slot given than it is connected to RSU R^* at the beginning. The P_{RC} of the reference vehicular node moving with a speed of V km/h can be expressed as a function of r and main-lobe beam width of RSU (ψ_M) as

$$\begin{aligned} P_{RC} &\overset{(a)}{=} \mathbb{P}[T_I > T_S] \overset{(b)}{=} \mathbb{P}[VT_S < D(r)] \\ &\overset{(c)}{=} \mathbb{P}\left[r > \frac{VT_S}{sin(\psi_M/2)} \left(\frac{W}{r} sin(\eta) + \sqrt{1 - \left(\frac{W}{r}\right)^2} \times cos(\eta) \right) \right]. \end{aligned} \tag{16}$$

The step (a) expressed the P_{RC} in terms of T_S and T_L, where T_L defines the maximum duration over which the vehicular node can remains connected to its serving RSU. P_{RC} is the probability that T_L is greater than T_S. The conditional probability, P_{RC} can also be expressed in terms of distance covered by vehicular node, as in step (b). It is the probability with which the vehicular node does not cover a distance greater than $D(r)$ within the slot, where $D(r)$ defines the maximum distance that the vehicular node can cover before leaving the communication range of its serving RSU. The expression in step (c) is followed from the Theorem 2 of reference [10], where $\eta = \pi/2 - \psi_M/2$. Note that, the resultant expression is a function of r, V, T_S, W, and ψ_M. where $\eta = \pi/2 - \psi_M/2$. Let $P_{RC,m}$ denotes the conditional probability with which the

[5]Slot duration defines the duration over which the beam configuration of RSU is kept fixed.

vehicular node remains connected to its mmWave RSU for the complete duration of considered slot given that it is connected to mmWave RSU at the beginning, and is given by

$$P_{RC,m} = P_{RC}, \tag{17}$$

where, ψ_M is small enough to perform directional beamforming to compensate for the high path loss at mmWave. For the microwave RSU, ψ_M is assumed to be 180°, since the microwave RSU are deployed at the side of the roads, and they are responsible for providing coverage only in one direction with a beam angle of 180°. By setting, $\psi_M = \pi$ in (16), and after some algebraic manipulation, the conditional probability with which the vehicular node remains connected to its microwave RSU for the complete duration of considered slot given than it is connected to microwave RSU at the beginning is given by

$$P_{RC,\mu} = \mathbb{P}\Big[r^2 > VT_S(\sqrt{r^2 - W^2})\Big]. \tag{18}$$

For the hybrid vehicular network, the connection probability is given by

$$P_{conn,PS} = P_{cov,m,PS}P_{RC,m} + P_{cov,\mu,PS}P_{RC,\mu}, \tag{19}$$

where, $P_{cov,m,PS}$ and $P_{cov,\mu,PS}$ are given in (13) and (14), respectively, while $P_{RC,m}$ and $P_{RC,\mu}$ are given by (17) and (18), respectively.

V. Spectral Efficiency Analysis

The spectral efficiency (or rate) for a vehicular node is defined as $\eta_S = \mathbb{E}[\ln(1 + \text{SINR})]$. We first obtain the average spectral efficiency expressions for a static vehicular node scenario. The spectral efficiency expressions for a static vehicular node can be obtained directly from coverage probability expressions by just replacing Υ_T with $\exp(t) - 1$, and then integrating the resulting expression over t [40]. Following this, the spectral efficiency expression for microwave network (denoted by $\eta_{S,\mu}$) and mmWave network (denoted by $\eta_{S,m}$) are given as:

$$\eta_{S,\mu} = \int_W^\infty \Big(\exp\Big\{\frac{-(\exp(t)-1){\sigma_\mu}^2}{P_t\hat{L}_1(\hat{r})}\Big\}\exp\{-2\lambda_\mu\hat{F}(\hat{r},t)\}\Big) \times f_\mu(\hat{r})d\hat{r}. \tag{20}$$

where $\hat{F}(\hat{r},t) = \int_{\hat{r}}^\infty \frac{(\exp(t)-1)\hat{L}_j(x)}{\hat{L}_1(\hat{r})+(e^t-1)\hat{L}_j(x)}dx$.

$$\eta_{S,m} = \int_W^\infty \Big(\exp\Big\{\frac{-(\exp(t)-1){\sigma_m}^2}{P_tL_1(r)}\Big\}\exp\{-2\lambda_m\hat{G}(r,t)\}\Big) \times f_M(r)dr, \tag{21}$$

where $\hat{G}(r,t) = \int_r^\infty \frac{G_IL_j(x)}{G_ML_1(r)+(\exp(t)-1)G_IL_j(x)}dx$.

In a similar fashion,, we can obtain the spectral efficiency expression for hybrid vehicular network. The spectral efficiency contributed by mmWave in hybrid vehicular network is given by

$$\eta_{S,PS,m} = \int_W^\infty \exp\Big\{\frac{-\max((\exp(t)-1),\Upsilon_{th}){\sigma_m}^2}{P_tL_1(r)}\Big\} \times\exp\{-2\lambda_m\hat{H}(r,t,\Upsilon_{th})\}f_M(r)dr. \tag{22}$$

$\hat{H}(r,t,\Upsilon_T,\Upsilon_{th}) = \int_r^\infty \frac{(\max(\exp(t)-1),\Upsilon_{th})G_IL_j(x)}{G_ML_1(r)+\max(\exp(t)-1),\Upsilon_{th})G_IL_j(x)}dx$.

The spectral efficiency contributed by microwave in hybrid vehicular network is given by (23), shown at the bottom of the next page. The effective spectral efficiency expression for the hybrid vehicular network can be obtained by adding (23) and (22).

A. Spectral Efficiency Analysis: Mobile Vehicular Node

In this subsection, we obtain the expression for the average spectral efficiency of a reference vehicular node moving with a speed of V km/h. Let T_{cov} represents the communication duration (i.e., fraction of slot duration) over which the reference vehicular node remains in the coverage range of its serving RSU. In this duration, the vehicular nodes can exchange data, on an average, with a spectral efficiency of η_S. Then, the average spectral efficiency over one slot is defined as

$$\eta_{mob} = \eta_S\frac{\mathbb{E}[T_{cov}]}{T_S}. \tag{24}$$

Note that, if reference vehicular node disconnected at the beginning of T_S, then $T_{cov} = 0$, hence $\eta_{mob} = 0$. However, if reference vehicular node connected at the beginning of T_S, then there may be two possibilities: (i) the reference vehicular node remains connected to serving RSU for the complete slot duration; we represent such a duration with $T_{cov,RC}$, (ii) the reference vehicular node remains connected to serving RSU for a fraction of slot duration; we represent such a duration with $T_{cov,DC}$. Accordingly, the average communication duration $\mathbb{E}[T_{cov}]$ can be expressed in terms of $T_{cov,RC}$ and $T_{cov,DC}$ as follows,

$$\mathbb{E}[T_{cov}] = P_{RC}\mathbb{E}[T_{cov,RC}] + (1 - P_{RC})\mathbb{E}[T_{cov,DC}], \tag{25}$$

while (25) can be expressed as a function of V and T_S using Lemma 3.

Lemma 3: The average communication duration over which the reference vehicular node remains in the coverage range of its serving RSU is expressed as:

$$\mathbb{E}[T_{cov}] = T_S - \frac{1}{V}\int_0^{VT_S} F_D(y)dy. \tag{26}$$

Proof: The first term in (25) represents the average duration over which the vehicular node remains connected to serving RSU for the complete slot duration with probability $P_{RC} = \mathbb{P}[d > VT_S]$, then $\mathbb{E}[T_{cov,RC}] = T_S$. While the

$$P_{cov,\mu,PS} = \int_W^\infty (1 - \exp\Big\{-\frac{\Upsilon_{th}{\sigma_m}^2}{P_tG_ML_1(r)}\Big\}\exp\{-2\lambda_mG(r,\Upsilon_{th})\})f_M(r)dr \times\int_W^\infty \exp\Big\{-\frac{\Upsilon_T{\sigma_\mu}^2}{P_t\hat{L}_1(\hat{r})}\Big\}\exp\{-2\lambda_{\mu,opt}F(\hat{r},\Upsilon_T)\}f_\mu^*(\hat{r})d\hat{r} \tag{14}$$

second term in (25) represents the average duration over which the vehicular node remains connected to serving RSU for a fraction of slot duration with probability $1 - P_{RC}$. $\mathbb{E}[T_{cov,DC}]$ can be expressed as a function of V and T_S as follows:

$$\begin{aligned}\mathbb{E}[T_{cov,DC}] &= \frac{\mathbb{E}[D(r)|D(r) < VT_S]}{V} \\ &\overset{(a)}{=} \frac{1}{V}\frac{\mathbb{E}(\mathbb{1}_{D(r)<VT_S}D(r))}{\mathbb{P}[D(r) < VT_S]} \\ &\overset{(b)}{=} \frac{1}{V}\frac{\int_0^{VT_S} y f_D(y)dy}{(1-P_{RC})} \\ &\overset{(c)}{=} \frac{1}{V}\frac{(VT_S)F_D(VT_S) - \int_0^{VT_S} F_D(y)dy}{(1-P_{RC})} \end{aligned} \tag{27}$$

Here step (a) follows from the definition of conditional expectation and from the condition $D(r) < VT_S$, where $\mathbb{1}_{D(r)<VT_S}$ is the indicator function, defined as follows:

$$\mathbb{1}_{D(r)<VT_S} = \begin{cases} 1 & \text{if } D(r) < VT_S, \\ 0 & \text{otherwise.} \end{cases} \tag{28}$$

The denominator in step (b) follows from Eq. (16), while the numerator in step (c) is obtained by solving the integral by parts, where $F_D(y)$ denotes the CDF of the distance $D(r)$. Now substituting the expression for $\mathbb{E}[T_{cov,DC}]$ from (27) and setting $\mathbb{E}[T_{cov,RC}] = T_S$ in (25), the simplified expression for $\mathbb{E}[T_{cov}]$ is given as

$$\mathbb{E}[T_{cov}] = P_{RC}T_S + \Big(T_S F_D(VT_S) - \frac{1}{V}\int_0^{VT_S} F_D(y)dy\Big). \tag{29}$$

Since $F_D(VT_S) = 1 - P_{RC}$, hence substituting it in (31) and after performing some algebraic manipulations, we get the resulting expression in (26). ∎

Now Eq. (24) can be renovated for mmWave and microwave network. The average spectral efficiency for mmWave network over one slot is defined as

$$\eta_{mob,m} = \eta_{S,m}\frac{\mathbb{E}[T_{cov,m}]}{T_S}. \tag{30}$$

where $\eta_{S,m}$ is given by Eq. (22) of manuscript, while the expression for $\mathbb{E}[T_{cov,m}]$ is followed from Eqs. (26)-(31), which is given by

$$\mathbb{E}[T_{cov,m}] = T_S - \frac{1}{V}\int_0^{VT_S} F_{D,m}(y)dy. \tag{31}$$

Similarly, the average spectral efficiency for microwave network over one slot is defined as

$$\eta_{mob,\mu} = \eta_{S,\mu}\frac{\mathbb{E}[T_{cov,\mu}]}{T_S}. \tag{32}$$

where $\eta_{S,\mu}$ is given by Eq. (20) of manuscript, while the expression for $\mathbb{E}[T_{cov,\mu}]$ is followed from Eqs (26)-(31), hence the resultant expression is given by:

$$\mathbb{E}[T_{cov,\mu}] = T_S - \frac{1}{V}\int_0^{VT_S} F_{D,\mu}(y)dy. \tag{33}$$

Next, we obtain the average spectral efficiency for hybrid vehicular network under mobile vehicular node scenario. The average spectral efficiency for hybrid vehicular network over one slot is defined as

$$\eta_{mob,PS} = \eta_{S,PS,m}\frac{\mathbb{E}[T_{cov,m}]}{T_S} + \eta_{S,PS,\mu}\frac{\mathbb{E}[T_{cov,\mu}]}{T_S}. \tag{34}$$

The first term in (34) defines the spectral efficiency contributed by mmWave RSU in hybrid vehicular network under a mobile vehicular node scenario. While the second term defines the spectral efficiency contributed by microwave RSU in hybrid vehicular network under a mobile vehicular node scenario. The expressions for $\eta_{S,PS,m}$ and $\eta_{S,PS,\mu}$ are given by Eq. (24) and Eq. (26), respectively in the revised manuscript. While, the expressions for $\mathbb{E}[T_{cov,m}]$ and $\mathbb{E}[T_{cov,\mu}]$ are given by (31) and (32), respectively. Hence, by substituting these expression into (34), one can obtain the final expression of average spectral efficiency for hybrid vehicular network.

VI. Energy Efficiency Analysis

In this section, we analyze the energy efficiency (nats/Hz/Joule) of hybrid vehicular network. Energy efficiency is defined as the ratio of total average spectral efficiency to the total power consumption [41]. Essentially, there are two sources for the total RSU power consumption: transmission power consumption (P_t) and circuit power consumption (P_c), which is given by [16],

$$P_T = \frac{P_t}{\rho} + P_c, \tag{35}$$

where, ρ denotes the efficiency of power amplifier. The major constitutes for the circuit power consumption are radio frequency (RF) chains. analog-to-digital converter (ADC), baseband signal processing, cooling, etc [42]. The circuit power consumption is given by

$$P_{ckt} = N_t P_{RF} + P_m + P_{ADC}. \tag{36}$$

Here, N_t denotes the number of antennas at RSU, P_{RF} denotes the power consumption due to RF chain, while P_{ADC} denotes the power consumption due to ADC, and is given by $P_{ADC} = cB$ [43], where B is the signal bandwidth, while the factor c depends on gate-oxide capacitance (c_{ox}) and quantization rate ($2^{R_{ADC}}$) of ADC, and is given by $a = c_{ox}2^{R_{ADC}}$. P_m denotes the other miscellaneous circuit power consumption that includes base-band processing, battery backup, cooling, etc. The power consumption due to ADC has considerable impact on circuit power consumption, especially for mmWave,

$$\begin{aligned}\eta_{S,PS,\mu} = &\int_W^\infty (1 - \exp\Big\{-\frac{\Upsilon_{th}{\sigma_m}^2}{P_t G_M L_1(r)}\Big\}\exp\{-2\lambda_m G(r,\Upsilon_{th})\})f_M(r)dr \\ &\times \int_W^\infty \exp\Big\{-\frac{(e^t-1){\sigma_\mu}^2}{P_t \hat{L}_1(\hat{r})}\Big\}\exp\{-2\lambda_{\mu,opt}F(\hat{r},t)\}f_\mu^*(\hat{r})d\hat{r}\end{aligned} \tag{23}$$

since it increases linearly with the bandwidth, thereby limit the full utilization of available bandwidth at mmWave frequency. Let $P_{ckt,m}$ and $P_{ckt,\mu}$ denote the total circuit power consumption due to mmWave RSU and microwave RSU, then the total power consumption due to mmWave RSU, and microwave RSU is given by

$$P_{T,m} = \frac{P_{t,m}}{\rho_m} + P_{ckt,m}, \quad P_{T,\mu} = \frac{P_{t,\mu}}{\rho_\mu} + P_{ckt,\mu}, \tag{37}$$

respectively. The energy spectral efficiency for mmWave vehicular network can be defined as [41],

$$\eta_{ES,m} = \frac{\eta_{S,m}}{P_{T,m}}. \tag{38}$$

In a similar manner, we can define the energy spectral efficiency for microwave vehicular network as

$$\eta_{ES,\mu} = \frac{\eta_{S,\mu}}{P_{T,\mu}}. \tag{39}$$

The energy spectral efficiency for hybrid vehicular network can be defined as [44],

$$\eta_{ES,PS} = \frac{\eta_{S,PS,m} + \eta_{S,PS,\mu}}{P_{T,m} + P_{T,\mu}}. \tag{40}$$

Using (22) and (23) in (40), we can obtain the expression of energy spectral efficiency for the hybrid vehicular network.

VII. Results and Discussion

In this section, we provide the simulations to validate the obtained analytical expressions. We perform the Monte-Carlo simulations in MATLAB to obtain the results, where each simulation point is an average result of 10^5 iterations. For the simulation, we consider 14.8 m wide road, which is divided into 4 equal width lanes. We model the obstacles in the outermost lanes using the practical probabilistic model as in [10], [38]. The mmWave and microwave RSU are distributed based on 1-D PPP at either side of the road. A reference vehicular node is considered at the center of the road (i.e., at the origin of the road). For the modeled network, we analyzed the performance in terms of coverage probability, connectivity probability, average rate, and energy efficiency. Also we compared these results with the mmWave vehicular network. Note that the results plotted for mmWave vehicular network will match the results of the papers [10], [17] for the same parameter settings. For the simulation of coverage probability, we first compute the SINR experienced by a reference vehicular node from the nearest mmWave RSU and check whether it is above the SINR threshold, Υ_{th}. If SINR $>$ Υ_{th}, the reference vehicular node would associate to mmWave RSU, otherwise the reference vehicular node would associate to microwave RSU. Then, the coverage probability is calculated by comparing the received SINR corresponding to associated RSU (mmWave or microwave) with target SINR (Υ_T). If SINR $> \Upsilon_T$, the reference vehicular node is considered to be in coverage. For the simulation of connectivity probability, we assume that the reference vehicular node is connected to a serving RSU R^* at the beginning of a time slot. Now, P_{NL} models the probability that the vehicle remains connected to its serving RSU. Then, we check whether our reference vehicular node, that moves at a speed of V km/h, is still able to connect to RSU R^* after a slot of duration T_S. In order to verify so, we compute the SINR experienced by a reference vehicular node from the connected RSU R^* (considering the new value of the distance between the reference vehicular node and RSU R^* at the end of the slot) and see if it is above the Υ_T. If SINR $>$ Υ_T, connection is maintained, meaning that the vehicle has not left the communication range of its serving RSU R^*. The spectral efficiency (η_S) of the hybrid vehicular network is calculated according to the Shannon formula (i.e., using the relation $\eta_S = \mathbb{E}[\ln(1 + \text{SINR})]$. The energy efficiency of the hybrid vehicular network is calculated by dividing the spectral efficiency by total RSU power consumption. The parameter values for simulations are listed in Table II unless stated separately.

TABLE II
Simulation Parameters

Parameters	Value
f_m	28 GHz
f_μ	2 GHz
F_m, F_μ	100 MHz, 10 MHz
P_m, P_μ	30 dBm, 46 dBm,
$\alpha_{\mu,L}$; $\alpha_{\mu,NL}$	2.09, 3.75
$\alpha_{m,L}$; $\alpha_{m,NL}$	2, 4
$2W$, L	14.8 m, 10 km
Number of lanes(N_l)	4
G_M, G_m, ψ_M	18 dBi, -2 dBi, 10
Microwave band antenna gain	0 dBi
h_O, H_U	1 m, 12 m
Noise power density (N_0)	-174 dBm/Hz
σ_m^2, σ_μ^2	$N_0 B_m$, $N_0 B_\mu$
λ_O	1
V	30 km/h, 100 km/h
P_{ADC}	$a \times Bandwidth$, where $a = 10^{-7}$

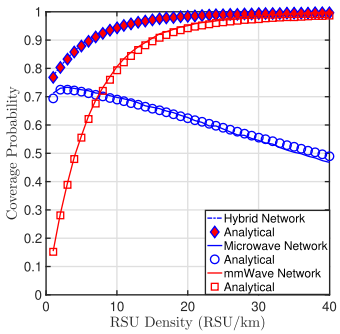

Fig. 4. Coverage probability versus RSU density (RSU/km) for mmWave, microwave and hybrid vehicular networks. Here, $T = 0$ dB, $\lambda_\mu = 3$ RSU/km for hybrid network.

A. Coverage Analysis

Fig. 4 shows the variation of coverage probability with respect to RSU density for mmWave, microwave, and hybrid vehicular networks. Note that for mmWave and hybrid networks, this RSU density is corresponding to mmWave RSU density, while for microwave network, the RSU density considered on x-axis is corresponding to microwave RSU density. It can be seen that, for microwave vehicular network, the

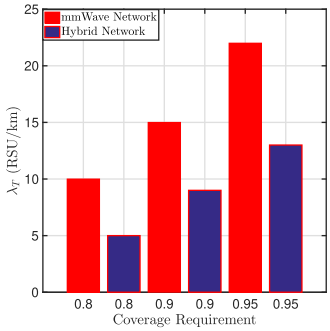

Fig. 5. A bar graph illustrating the total numbers of RSU required for a fixed coverage requirement by mmWave and hybrid networks.

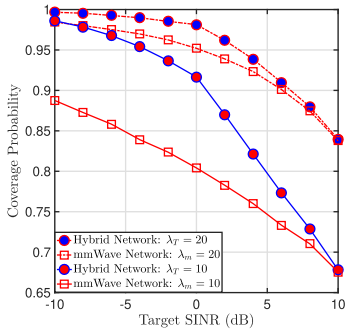

Fig. 6. Coverage probability versus T for mmWave, and hybrid vehicular network. Here, $\lambda_\mu = 3$ RSU/km for hybrid network.

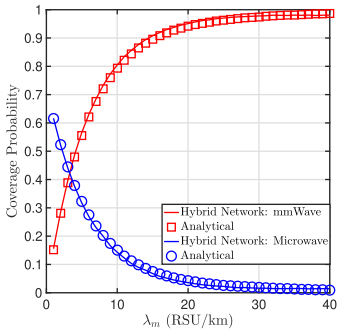

Fig. 7. Illustration of individual contribution by mmWave and microwave RSU in the hybrid vehicular network.

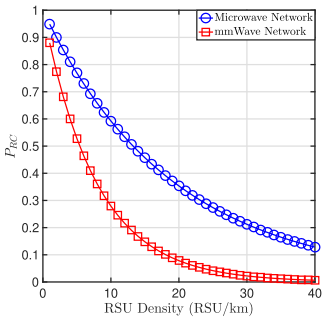

Fig. 8. The variation of conditional connectivity probability vs RSU density (RSU/km) for microwave and mmWave vehicular networks.

coverage probability initially increases with the increase in RSU density, where the signal power dominates the interference power and attains a maximum value for the RSU density governed by (9). With further increase in density of the microwave RSU, the coverage probability starts decreasing, since the interference power starts dominating the signal power. The density at which coverage is maximum is regarded as the optimum value of the microwave RSU density. For mmWave RSU, the coverage probability first increases with the increase in mmWave RSU density. Then, with further increase in density of mmWave RSU, the coverage probability saturate to a fixed value. For the analysis of the hybrid vehicular network, the density of microwave RSU is set to an optimum value, while we vary the mmWave RSU density and observe the coverage probability. Here, the optimum microwave RSU density (λ_μ) is considered to be 3. It can be seen that the coverage probability increases with the mmWave RSU density. Further, it can be observed that the coverage probability of the hybrid vehicular network is always higher than the coverage probability of other two networks (i.e., mmWave and microwave networks). In other words, the hybrid vehicular network requires a lesser number of RSU in comparison to the mmWave vehicular network and microwave vehicular network for the same coverage probability requirements as shown in Fig. 5.

The bar graph shown in Fig. 5 illustrates the total number of RSU required corresponding to the prescribed coverage for mmWave and hybrid vehicular networks (which includes both the microwave and mmWave RSU). It can be seen that the hybrid vehicular network requires a lesser number of RSU in comparison to the mmWave vehicular network for the same coverage probability. The reason is that, hybrid network considers the combination of mmWave and microwave RSU, where the number of microwave RSU deployed in the hybrid network are based on the maximum coverage probability of the microwave network. The microwave network offers coverage over a long distance. Hence, the use of microwave RSU in hybrid network significantly reduces the number of mmWave RSU required in hybrid network compared to the mmWave network for similar coverage probability.

Fig. 6 compares the coverage performance of the mmWave and hybrid vehicular network with respect to the target SINR for $\lambda_T = 10$ and $\lambda_T = 20$. Note that λ_T denotes the total RSU density in hybrid vehicular network, which includes both the mmWave RSU density, λ_m and microwave RSU density, λ_μ, where λ_μ is considered to be 3. It can be seen that the hybrid vehicular network has higher coverage probability than the mmWave vehicular network. Moreover, it can be observed that the difference in that coverage probability is significant at lower values of the target SINR.

Fig. 7 depicts the individual coverage contributed by mmWave and microwave RSU in the hybrid vehicular network. It can be seen that the contribution of the mmWave RSU in the coverage probability increases with the increase in the mmWave RSU density, since the increase in mmWave RSU density reduces the distance between reference vehicular node and serving RSU. Hence the coverage probability contributed by microwave RSU decreases. In other words, the load on the microwave RSU for contribution in the coverage probability reduces with the increase in mmWave RSU density.

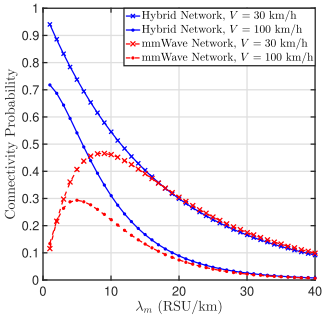

(a) For different values of V with parameters $T_S = 1$ sec, $\psi_M = 10^\circ$.

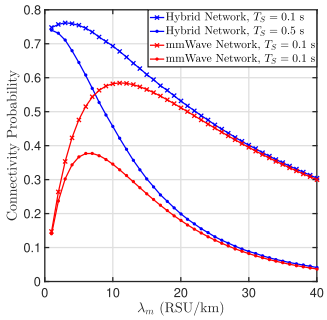

(b) For different values of T_S with parameters $V = 100$ km/h, $\psi_M = 10^\circ$.

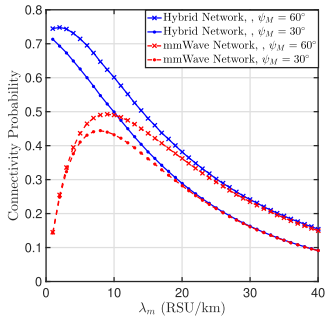

(c) For different values of ψ_M with parameters $T_S = 1$ sec, $V = 60$ km/h.

Fig. 9. Connectivity probability versus λ_m for mmWave and hybrid vehicular network.

B. Connectivity Analysis

Fig. 8 compares the P_{RC} with respect to RSU density for mmWave and microwave vehicular network. The following observations can be made from these results. First, it can be observed that, P_{RC} decreases with RSU density. The reason is that, in denser scenario, the distance r between reference vehicular node and serving RSU decreases, consequently the maximum distance that the vehicular node can cover before leaving the communication range of its associated RSU decreases. In other words, P_{RC} decreases with densification of RSU. Second, it can be observed that, microwave vehicular network has higher P_{RC} than mmWave vehicular network. The reason is that, the microwave RSU employs a much wider beam than the mmWave RSU to serve the vehicular nodes. The wider beams increase the coverage area of vehicular node from its serving RSU, hence guaranteeing more durable association within the slot.

Fig. 9 shows the variation in connectivity probability with respect to the mmWave RSU density for the mmWave and the hybrid vehicular network. The results are shown for three different system configurations. The following common observations can be made from all these system configurations. First, it can be observed that the hybrid vehicular network has a higher connectivity probability than the mmWave vehicular network. The reason is that the hybrid vehicular network employs both the mmWave and microwave networks, where microwave networks has higher P_{RC} than the mmWave networks as depicted in Fig. 9. Note that the difference in the connectivity probability is significant at a lower mmWave RSU density. However, this difference decreases with increase in mmWave RSU density. This is because, with the increase in mmWave RSU density, contribution by microwave RSU decreases. In such a case, the microwave RSU only serves the purpose of a backup link in the scenarios where mmWave RSU are not sufficient to serve the vehicular node due to blockage effect. Fig. 9 (a) shows the variation in connectivity probability with respect to the mmWave RSU density for different vehicle velocity. It can be seen that slow-moving vehicles have higher connectivity probability than fast-moving vehicles because the slow-moving vehicles covers comparatively larger distance than the fast-moving vehicles within one slot. Fig. 9 (b) depicts the variation in connectivity probability with respect to the mmWave RSU density for different values of time-slot. It is shown that connectivity probability increases with the decrease in time-slot, since the beam alignment is repeated more frequently, hence the disconnection probability is reduced. Fig. 9 (c) shows that connectivity probability increases with ψ_M, since the broader beams widen the area, hence reduces the probability for the vehicular node to get disconnect from its serving RSU.

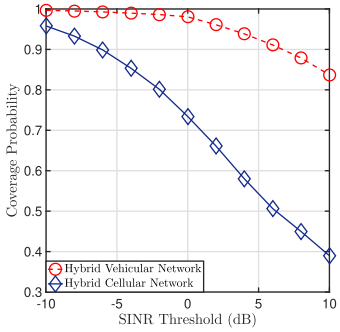

Fig. 10. Coverage probability comparison of hybrid vehicular and hybrid cellular network. Here, $\lambda_T = 20$ RSU/km, $\Upsilon_{th} = -5$ dB.

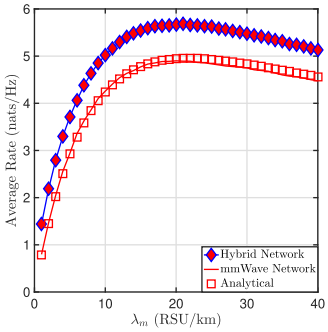

Fig. 11. Spectral efficiency variation with respect to mmWave RSU density for mmWave and hybrid vehicular network.

Fig. 10 compares the coverage probability of hybrid vehicular network with hybrid cellular network [33]. To perform the simulations for the hybrid cellular networks, we model the two-tier network, with first-tier of sparsely deployed microwave base station (BS) and second-tier of densely deployed mmWave BS. The hybrid cellular network [33]

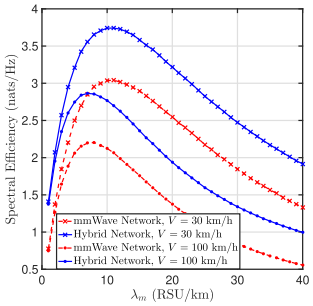

(a) For different values of V with parameters $T_S = 1$ sec, $\psi_M = 10°$.

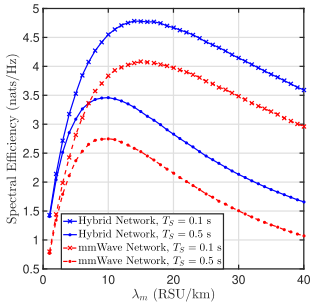

(b) For different values of T_S with parameters $V = 100$ km/h, $\psi_M = 10°$.

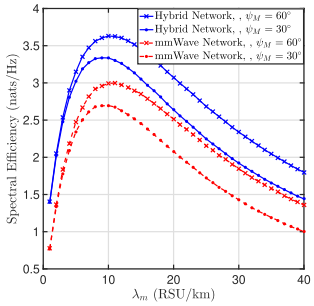

(c) For different values of ψ_M with parameters $T_S = 1$ sec, $V = 100$ km/h.

Fig. 12. Spectral efficiency variation with respect to λ_m for mmWave and hybrid vehicular network under mobile vehicular node scenario.

considered a maximum received power based association strategy, that is, the user is associated to either nearest mmWave or nearest microwave BS for which the received signal is maximum. The parameters are kept same as of hybrid vehicular network. It can be observed that, hybrid vehicular network has high coverage probability than hybrid cellular network.

C. Spectral Efficiency and Energy Efficiency Analysis

Fig. 11 compares the spectral efficiency (nats/Hz) for the mmWave vehicular network and the hybrid vehicular networks. It can be seen that the hybrid vehicular network has higher average rate than the mmWave vehicular network. The reason is the noise power increases linearly with the bandwidth (B) as noise power $P_n = N_0 B$, where N_0 denotes the noise power spectral density. It leads to a reduction in SINR for a wide-band mmWave network. Hence, mixing the narrow-band microwave network with mmWave network leads to improve in average rate of the hybrid vehicular network.

Fig. 12 shows the variation of spectral efficiency with respect to λ_m for mmWave and hybrid vehicular network under mobile vehicular node scenario. We vary λ_m and plot the spectral efficiency curves for different system configurations. It can be observed that, spectral efficiency follows the same trend for all configurations. In particular, the trend is similar to the spectral efficiency analysis under static vehicular node scenario, that is, the spectral efficiency increases with λ_m for sparse networks, however after some density threshold, spectral efficiency decreases. Moreover, it can be observed that, the hybrid vehicular network has higher spectral efficiency than the mmWave vehicular network. Fig. 12 (a) shows that the spectral efficiency increases as velocity decreases, because the probability of disconnecting the vehicular node from its serving RSU during the slot decreases. Similarly, Fig. 12 (b) shows that the spectral efficiency increases with decreasing time slots, as the beam alignment is repeated more frequently, hence the disconnection time is reduced. From Fig. 12 (c), it can be noticed that spectral efficiency increases with ψ_M, since the broader beams widen the area in which the vehicular node can get coverage from its serving RSU.

Fig. 13 depicts the variation in spectral efficiency with respect to Υ_{th} for the hybrid vehicular network. It can be seen that spectral efficiency for the hybrid vehicular network

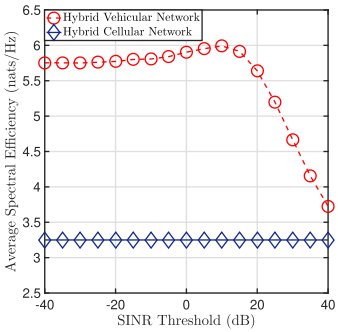

Fig. 13. Average spectral efficiency variation with respect to Υ_{th} for hybrid vehicular network and hybrid cellular network.

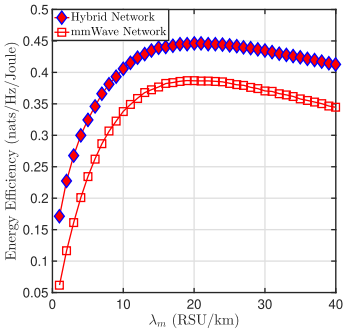

Fig. 14. Energy spectral efficiency variation with respect to mmWave RSU density for mmWave and hybrid vehicular network.

increases gradually with the increase in Υ_{th}. However, above a certain Υ_{th}, spectral efficiency decreases sharply. The reason is as follows: for smaller value of Υ_{th}, the most of the vehicular nodes get served by mmWave RSU, while for larger value of Υ_{th}, the most of the vehicular nodes get served by microwave RSU. Furthermore, the number of mmWave RSU deployed are more than the microwave RSU, hence the average spectral efficiency contributed by mmWave RSU is more than the microwave RSU. In between these two extreme values, the vehicular nodes get served by both the mmWave and microwave RSU, and the spectral efficiency attains a maximum value for particular Υ_{th} threshold, where both the mmWave and microwave RSU efficiently utilizes their resources to serve the vehicular nodes. Moreover, the plots compare the

spectral efficiency of hybrid vehicular network with the hybrid cellular network. It can be observed that the hybrid vehicular network has higher spectral efficiency than the hybrid cellular network, as the association strategy for the hybrid vehicular network is based on SINR, rather on the received power for hybrid cellular network. Furthermore, the association strategy for a hybrid vehicular network prioritizes the association of reference vehicular node with mmWave RSU based on Υ_{th}.

Fig. 14 compares the energy efficiency (nats/Hz/watt) for the mmWave and hybrid vehicular network. It can be observed that hybrid vehicular network has higher energy efficiency than the mmWave vehicular network because hybrid vehicular network has higher spectral efficiency than the mmWave vehicular network as depicted in Fig. 11. Moreover, the circuit power consumption due to ADC is a decreasing function of bandwidth, that is, the circuit power is significantly high for mmWave networks. Consequently, the hybrid vehicular network, that employs both mmWave and microwave networks, has comparatively less circuit power consumption than the mmWave networks.

VIII. Conclusion

In this work, we consider the downlink vehicular communication scenario, where both the mmWave and microwave interfaces are used together. The performance of such a scenario is analyzed in terms of coverage probability, connectivity, and energy efficiency of the system and compared these analysis with the existing mmWave vehicular communication scenario and microwave vehicular communication scenario. It is concluded that hybrid vehicular network ensures high reliability (in terms of coverage) of the system. In future work, the performance of the hybrid vehicular network would be analyzed on upper layers network parameters, especially on the latency of the system.

Appendix A
Proof of Lemma 1

The average coverage probability for a reference vehicular node served by microwave RSU is given by

$$\begin{aligned} P_{cov,\mu} &= \int_W^\infty \mathbb{P}[\Upsilon_\mu > \Upsilon_T] f_\mu(\hat{r}) d\hat{r} \\ &\overset{(a)}{=} \int_W^\infty \mathbb{P}\Big[\frac{P_t \hat{g}_1 \hat{L}_1(\hat{r})}{\sigma_\mu^2 + I_\mu} > \Upsilon_T\Big] f_\mu(\hat{r}) d\hat{r} \\ &= \int_W^\infty \mathbb{P}\Big[\hat{g}_1 > \frac{\Upsilon_T(\sigma_\mu^2 + I_\mu)}{P_t \hat{L}_1(\hat{r})}\Big] f_\mu(\hat{r}) d\hat{r}. \quad (41) \end{aligned}$$

where (a) follows from (4) by substituting the expression of Υ_μ. Since $\hat{g}_1 \sim \exp(1)$, the probability term inside (41) can be written as

$$\begin{aligned} \mathbb{P}\Big[\hat{g}_1 > \frac{\Upsilon_T(\sigma_\mu^2 + I_\mu)}{P_t \hat{L}_1(\hat{r})}\Big] &= \exp\Big\{\frac{-\Upsilon_T \sigma_\mu^2}{P_t \hat{L}_1(\hat{r})}\Big\} \mathbb{E}_{I_\mu}\Big[\exp\Big\{\frac{-\Upsilon_T I_\mu}{P_t \hat{L}_1(\hat{r})}\Big\}\Big] \\ &= \exp\Big\{\frac{-\Upsilon_T \sigma_\mu^2}{P_t \hat{L}_1(\hat{r})}\Big\} \mathcal{L}_{I_\mu}\Big(\frac{\Upsilon_T}{P_t \hat{L}_1(\hat{r})}\Big), \quad (42) \end{aligned}$$

where $\mathcal{L}_{I_\mu(t)}$ is the Laplace transform of random variable I_μ evaluated at t and is given by

$$\begin{aligned} \mathcal{L}_{I_\mu(t)} &= \mathbb{E}_{I_\mu}[\exp\{-tI_\mu\}] = \mathbb{E}_{\xi_\mu, \hat{g}_j}\Big[\exp\{-t \sum_{j \in \xi_\mu} P_t \hat{g}_j \hat{L}_j(\hat{r})\}\Big] \\ &= \mathbb{E}_{\xi_\mu}\Big[\prod_{j \in \xi_\mu} \mathbb{E}_{\hat{g}_j}\big(\exp\{-tP_t \hat{g}_j \hat{L}_j(\hat{r})\}\big)\Big]. \quad (43) \end{aligned}$$

Since $\hat{g}_j \sim \exp(1)$, (43) can be expressed as

$$\begin{aligned} \mathcal{L}_{I_\mu}(t) &= \mathbb{E}_{\xi_\mu}\Big[\prod_{j \in \xi_\mu} \frac{1}{1 + tP_t \hat{L}_j(\hat{r})}\Big] \\ &\overset{(b)}{=} \exp\Big\{-2\lambda_\mu \int_{\hat{r}}^\infty \Big(1 - \frac{1}{1 + tP_t \hat{L}_j(x)} dx\Big)\Big\} \\ &\overset{(c)}{=} \exp\Big\{-2\lambda_\mu \int_{\hat{r}}^\infty \frac{tP_t \hat{L}_j(x)}{1 + tP_t \hat{L}_j(x)} dx\Big\}. \quad (44) \end{aligned}$$

Here (b) follows from the probability generating functional (PGFL) of 1-D PPP, while (c) is obtained after some algebraic manipulation. Substituting $t = \frac{\Upsilon_T}{P_t \hat{L}_1(\hat{r})}$ in (44), we get,

$$\begin{aligned} \mathcal{L}_{I_\mu}\Big(\frac{\Upsilon_T}{P_t \hat{L}_1(\hat{r})}\Big) &= \exp\Big\{-2\lambda_\mu \int_{\hat{r}}^\infty \frac{\Upsilon_T \hat{L}_j(x)}{\hat{L}_1(\hat{r}) + \Upsilon_T \hat{L}_j(x)} dx\Big\} \\ &= \exp\{-2\lambda_\mu F(\hat{r}, \Upsilon_T)\}, \quad (45) \end{aligned}$$

where $F(\hat{r}, \Upsilon_T) = \int_{\hat{r}}^\infty \frac{\Upsilon_T \hat{L}_j(x)}{\hat{L}_1(\hat{r}) + \Upsilon_T \hat{L}_j(x)} dx$. Substitute (45) in (42), and then substitute the resulting expression in (41), we get (8).

Appendix B
Proof of Lemma 2

The average coverage probability for a reference vehicular node served by mmWave RSU is given by

$$\begin{aligned} P_{cov,m} &= \int_W^\infty \mathbb{P}[\Upsilon_m > \Upsilon_T] f_M(r) dr \\ &= \int_W^\infty \mathbb{P}\Big[\frac{P_t g_1 G_M L_1(r)}{{\sigma_m}^2 + I_m} > \Upsilon_T\Big] f_M(r) dr \\ &= \int_W^\infty \mathbb{P}\Big[g_1 > \frac{\Upsilon_T({\sigma_m}^2 + I_m)}{P_m G_M L_1(r)}\Big] f_M(r) dr. \quad (46) \end{aligned}$$

Since $g_1 \sim \exp(1)$, the probability term inside (46) can be written as

$$\begin{aligned} &\mathbb{P}\Big[g_1 > \frac{\Upsilon_T({\sigma_m}^2 + I_m)}{P_t G_M L_1(r)}\Big] \\ &= \mathbb{E}_{I_m}\Big[\exp\Big\{\frac{-\Upsilon_T {\sigma_m}^2}{P_t G_M L_1(r)}\Big\} \times \exp\Big\{\frac{-\Upsilon_T I_m}{P_t G_M L_1(r)}\Big\}\Big] \\ &= \exp\Big\{\frac{-\Upsilon_T {\sigma_m}^2}{P_t G_M L_1(r)}\Big\} \mathcal{L}_{I_m}\Big(\frac{\Upsilon_T}{P_t G_M L_1(r)}\Big), \quad (47) \end{aligned}$$

where, the laplacian functional $\mathcal{L}_{I_m}(t)$ is given by

$$\begin{aligned} \mathcal{L}_{I_m}(t) &= \mathbb{E}_{I_m}[\exp\{-tI_m\}] = \mathbb{E}_{I_m}\Big[\exp\{-t \sum_{j \in \xi_m} P_t g_j G_I L_j(r)\}\Big] \\ &= \mathbb{E}_{\xi_m, g_j}\Big[\exp\{-t \sum_{j \in \xi_m} P_t g_j G_I L_j(r)\}\Big] \\ &= \mathbb{E}_{\xi_m}\Big[\prod_{j \in \xi_m} \mathbb{E}_{g_j}\big(\exp\{-tP_t g_j G_I L_j(r)\}\big)\Big]. \quad (48) \end{aligned}$$

Since $g_j \sim \exp(1)$, (48) can be expressed as,

$$\begin{aligned}\mathcal{L}_{I_m(t)} &= \mathbb{E}_{\xi_m}\Big[\prod_{j\in\xi_m^{\xi}}\frac{1}{1+tP_tG_IL_j(r)}\Big]\\ &\overset{(d)}{=} \exp\Big\{-2\lambda_m\int_r^{\infty}\Big(1-\frac{1}{1+tP_tG_IL_j(x)}dx\Big)\Big\}\\ &\overset{(e)}{=} \exp\Big\{-2\lambda_m\int_r^{\infty}\frac{tP_tG_IL_j(x)}{1+tP_tG_IL_j(x)}dx\Big\}. \end{aligned} \quad (49)$$

Here, (d) follows from the PGFL of the 1-D PPP, while (e) is obtained after some algebraic manipulation. Substitute $t = \frac{\Upsilon_T}{P_tG_ML_1(r)}$ in (49), we get,

$$\mathcal{L}_{I_m}\Big(\frac{\Upsilon_T}{P_mG_ML_1(r)}\Big) = \exp\{-2\lambda_m G(r,\Upsilon_T)\}, \quad (50)$$

where $G(r,\Upsilon_T) = \int_r^{\infty}\frac{\Upsilon_T G_IL_j(x)}{G_ML_1(r)+\Upsilon_T G_IL_j(x)}dx$.

Substitute (50) in (47), and then substitute back the resulting expression in (46), we obtain the average coverage probability expression for vehicular node served by mmWave RSU,which is given by (12).

Appendix C
Proof of Theorem 1

The average coverage probability contributed by mmWave RSU is given by,

$$\begin{aligned}P_{cov,m,PS} = \int_W^{\infty}&\{\mathbb{P}[\Upsilon_m > \Upsilon_T|\Upsilon_m > \Upsilon_{th}]\mathbb{P}(\Upsilon_m > \Upsilon_{th})\}\\ &\times f_M(r)dr. \end{aligned} \quad (51)$$

Upon applying Bayes' rule, (51) can be rewritten as

$$\begin{aligned}P_{cov,m,PS} &= \int_W^{\infty}\mathbb{P}[\Upsilon_m > \Upsilon_T, \Upsilon_m > \Upsilon_{th}]f_M(r)dr\\ &= \int_W^{\infty}\mathbb{P}[\Upsilon_m > \max(\Upsilon_T,\Upsilon_{th})]f_M(r)dr\\ &= \int_W^{\infty}\mathbb{P}\Big[g_1 > \frac{\max(\Upsilon_T,\Upsilon_{th})({\sigma_m}^2+I_m)}{P_tG_ML_1(r)}\Big]f_M(r)dr. \end{aligned} \quad (52)$$

Since $g_1 \sim \exp(1)$, the simplification of (52) follow the steps (46)-(50), just replace Υ_T with $\max(\Upsilon_T,\Upsilon_{th})$. The final expression for $P_{cov,m,PS}$ is given by

$$\begin{aligned}P_{cov,m,PS} = \int_W^{\infty}&\exp\Big\{\frac{-\max(\Upsilon_T,\Upsilon_{th}){\sigma_m}^2}{P_tG_ML_1(r)}\Big\}\\ &\times\exp\{-2\lambda_m H(r,\Upsilon_T,\Upsilon_{th})\}f_M(r)dr, \end{aligned} \quad (53)$$

where

$$H(r,\Upsilon_T,\Upsilon_{th}) = \int_r^{\infty}\frac{\max(\Upsilon_T,\Upsilon_{th})G_IL_j(x)}{G_ML_1(r)+\max(\Upsilon_T,\Upsilon_{th})G_IL_j(x)}dx. \quad (54)$$

Appendix D
Proof of Theorem 2

The coverage probability contributed by microwave RSU is given by

$$P_{cov,\mu,PS} = \mathbb{P}[\Upsilon_{\mu,opt} > \Upsilon_T|\Upsilon_m < \Upsilon_{th}](1-\mathbb{P}(\Upsilon_m > \Upsilon_{th})). \quad (55)$$

Upon applying Bayes' rule and under the assumption of g_1 and $\hat{g}_1$ are i.i.d., (55) can be rewritten as

$$P_{cov,\mu,PS} = \mathbb{P}[\Upsilon_{\mu,opt} > \Upsilon_T](1-\mathbb{P}(\Upsilon_m > \Upsilon_{th})). \quad (56)$$

Here, the first term in (56) i.e., $\mathbb{P}[\Upsilon_{\mu,opt} > \Upsilon_T]$ follows from Lemma 1 and (10), while the second term in (56) i.e., $\mathbb{P}(\Upsilon_m > \Upsilon_{th})$ follows from Lemma 2. The final resulting expression is given by

$$\begin{aligned}P_{cov,\mu,PS} = \exp&\Big\{-\frac{\Upsilon_T{\sigma_\mu}^2}{P_t\hat{L}_1(\hat{r})}\Big\}\exp\{-2\lambda_{\mu,opt}F(\hat{r},\Upsilon_T,..)\}\\ &\times\Big(1-\exp\Big\{-\frac{\Upsilon_{th}{\sigma_m}^2}{P_tG_ML_1(r)}\Big\}\exp\{-2\lambda_m G(r,\Upsilon_T)\}\Big). \end{aligned} \quad (57)$$

The average coverage probability contributed by microwave RSU in the hybrid vehicular network can be obtained by averaging the resulting expression (57) over its pdf, which is given by (14).

References

[1] G. Karagiannis *et al.*, "Vehicular networking: A survey and tutorial on requirements, architectures, challenges, standards and solutions," *IEEE Commun. Surveys Tuts.*, vol. 13, no. 4, pp. 584–616, 4th Quart., 2011.

[2] J. Wang, J. Liu, and N. Kato, "Networking and communications in autonomous driving: A survey," *IEEE Commun. Surveys Tuts.*, vol. 21, no. 2, pp. 1243–1274, 2nd Quart., 2019.

[3] R. Kulandaivel, M. Balasubramaniam, F. Al-Turjman, L. Mostarda, M. Ramachandran, and R. Patan, "Intelligent data delivery approach for smart cities using road side units," *IEEE Access*, vol. 7, pp. 139462–139474, 2019.

[4] Y. Ren, R. Werner, N. Pazzi, and A. Boukerche, "Monitoring patients via a secure and mobile healthcare system," *IEEE Wireless Commun.*, vol. 17, no. 1, pp. 59–65, Feb. 2010.

[5] V. Oleshchuk and R. Fensli, "Remote patient monitoring within a future 5G infrastructure," *Wireless Pers. Commun.*, vol. 57, no. 3, pp. 431–439, Apr. 2011, doi: 10.1007/s11277-010-0078-5.

[6] J. Shi, Z. Yang, H. Xu, M. Chen, and B. Champagne, "Dynamic resource allocation for LTE-based Vehicle-to-Infrastructure networks," *IEEE Trans. Veh. Technol.*, vol. 68, no. 5, pp. 5017–5030, May 2019.

[7] G. Araniti, C. Campolo, M. Condoluci, A. Iera, and A. Molinaro, "LTE for vehicular networking: A survey," *IEEE Commun. Mag.*, vol. 51, no. 5, pp. 148–157, May 2013.

[8] J. Choi, V. Va, N. Gonzalez-Prelcic, R. Daniels, C. R. Bhat, and R. W. Heath, Jr., "Millimeter-wave vehicular communication to support massive automotive sensing," *IEEE Commun. Mag.*, vol. 54, no. 12, pp. 160–167, Dec. 2016.

[9] S. Chen *et al.*, "Vehicle-to-everything (v2x) services supported by LTE-based systems and 5G," *IEEE Commun. Standards Mag.*, vol. 1, no. 2, pp. 70–76, 2017.

[10] M. Giordani, M. Rebato, A. Zanella, and M. Zorzi, "Coverage and connectivity analysis of millimeter wave vehicular networks," *Ad Hoc Netw.*, vol. 80, pp. 158–171, Nov. 2018.

[11] S.-H. Sun, J.-L. Hu, Y. Peng, X.-M. Pan, L. Zhao, and J.-Y. Fang, "Support for vehicle-to-everything services based on LTE," *IEEE Wireless Commun.*, vol. 23, no. 3, pp. 4–8, Jun. 2016.

[12] S. Chen, J. Hu, Y. Shi, and L. Zhao, "LTE-V: A TD-LTE-based V2X solution for future vehicular network," *IEEE Internet Things J.*, vol. 3, no. 6, pp. 997–1005, Dec. 2016.

[13] H. Seo, K.-D. Lee, S. Yasukawa, Y. Peng, and P. Sartori, "LTE evolution for vehicle-to-everything services," *IEEE Commun. Mag.*, vol. 54, no. 6, pp. 22–28, Jun. 2016.

[14] T.-J. Wu, W. Liao, and C.-J. Chang, "A cost-effective strategy for road-side unit placement in vehicular networks," *IEEE Trans. Commun.*, vol. 60, no. 8, pp. 2295–2303, Aug. 2012.

[15] F. Jiang, C. Li, and Z. Gong, "Low complexity and fast processing algorithms for V2I massive MIMO uplink detection," *IEEE Trans. Veh. Technol.*, vol. 67, no. 6, pp. 5054–5068, Jun. 2018.

[16] M. Patra, R. Thakur, and C. S. R. Murthy, "Improving delay and energy efficiency of vehicular networks using mobile femto access points," *IEEE Trans. Veh. Technol.*, vol. 66, no. 2, pp. 1496–1505, Feb. 2017.

[17] A. Tassi, M. Egan, R. J. Piechocki, and A. Nix, "Modeling and design of millimeter-wave networks for highway vehicular communication," *IEEE Trans. Veh. Technol.*, vol. 66, no. 12, pp. 10676–10691, Dec. 2017.
[18] J. Chen, G. Mao, C. Li, A. Zafar, and A. Y. Zomaya, "Throughput of infrastructure-based cooperative vehicular networks," *IEEE Trans. Intell. Transp. Syst.*, vol. 18, no. 11, pp. 2964–2979, Nov. 2017.
[19] Y. Wang, K. Venugopal, A. F. Molisch, and R. W. Heath, Jr., "MmWave Vehicle-to-Infrastructure communication: Analysis of urban microcellular networks," *IEEE Trans. Veh. Technol.*, vol. 67, no. 8, pp. 7086–7100, Aug. 2018.
[20] C. Xu, C. Gao, Z. Zhou, Z. Chang, and Y. Jia, "Social network-based content delivery in device-to-device underlay cellular networks using matching theory," *IEEE Access*, vol. 5, pp. 924–937, 2017.
[21] Z. Zhou, H. Yu, C. Xu, Y. Zhang, S. Mumtaz, and J. Rodriguez, "Dependable content distribution in D2D-based cooperative vehicular networks: A big data-integrated coalition game approach," *IEEE Trans. Intell. Transp. Syst.*, vol. 19, no. 3, pp. 953–964, Mar. 2018.
[22] Z. Zhou, H. Liao, X. Zhao, B. Ai, and M. Guizani, "Reliable task offloading for vehicular fog computing under information asymmetry and information uncertainty," *IEEE Trans. Veh. Technol.*, vol. 68, no. 9, pp. 8322–8335, Sep. 2019.
[23] B. Gu and Z. Zhou, "Task offloading in vehicular mobile edge computing: A matching-theoretic framework," *IEEE Veh. Technol. Mag.*, vol. 14, no. 3, pp. 100–106, Sep. 2019.
[24] V. V. Chetlur and H. S. Dhillon, "Coverage and rate analysis of downlink cellular vehicle-to-everything (C-V2X) communication," *IEEE Trans. Wireless Commun.*, vol. 19, no. 3, pp. 1738–1753, Mar. 2020.
[25] X. Ge, "Ultra-reliable low-latency communications in autonomous vehicular networks," *IEEE Trans. Veh. Technol.*, vol. 68, no. 5, pp. 5005–5016, May 2019.
[26] H. Khan, S. Samarakoon, and M. Bennis, "Enhancing video streaming in vehicular networks via resource slicing," *IEEE Trans. Veh. Technol.*, vol. 69, no. 4, pp. 3513–3522, Apr. 2020.
[27] X. Song and M. Yuan, "Performance analysis of one-way highway vehicular networks with dynamic multiplexing of eMBB and URLLC traffics," *IEEE Access*, vol. 7, pp. 118020–118029, 2019.
[28] H. Yang, K. Zheng, L. Zhao, and L. Hanzo, "Twin-timescale radio resource management for ultra-reliable and low-latency vehicular networks," *IEEE Trans. Veh. Technol.*, vol. 69, no. 1, pp. 1023–1036, Jan. 2020.
[29] O. Semiari, W. Saad, M. Bennis, and M. Debbah, "Integrated millimeter wave and sub-6 GHz wireless networks: A roadmap for joint mobile broadband and ultra-reliable low-latency communications," *IEEE Wireless Commun.*, vol. 26, no. 2, pp. 109–115, Apr. 2019.
[30] O. Semiari, W. Saad, and M. Bennis, "Joint millimeter wave and microwave resources allocation in cellular networks with dual-mode base stations," *IEEE Trans. Wireless Commun.*, vol. 16, no. 7, pp. 4802–4816, Jul. 2017.
[31] G. Ghatak, A. De Domenico, and M. Coupechoux, "Modeling and analysis of HetNets with mm-Wave multi-RAT small cells deployed along roads," in *Proc. GLOBECOM IEEE Global Commun. Conf.*, Dec. 2017, pp. 1–7.
[32] M. Shi, K. Yang, C. Xing, and R. Fan, "Decoupled heterogeneous networks with millimeter wave small cells," *IEEE Trans. Wireless Commun.*, vol. 17, no. 9, pp. 5871–5884, Sep. 2018.
[33] M. Shi, K. Yang, Z. Han, and D. Niyato, "Coverage analysis of integrated sub-6 GHz-mmWave cellular networks with hotspots," *IEEE Trans. Commun.*, vol. 67, no. 11, pp. 8151–8164, Nov. 2019.
[34] Q. Hu, C. Wu, X. Zhao, X. Chen, Y. Ji, and T. Yoshinaga, "Vehicular multi-access edge computing with licensed sub-6 GHz, IEEE 802.11p and mmWave," *IEEE Access*, vol. 6, pp. 1995–2004, 2018.
[35] X. Zhang, Y. Li, and Q. Miao, "A cluster-based broadcast scheduling scheme for mmWave vehicular communication," *IEEE Commun. Lett.*, vol. 23, no. 7, pp. 1202–1206, Jul. 2019.
[36] A. K. Gupta, J. G. Andrews, and R. W. Heath, Jr., "On the feasibility of sharing spectrum licenses in mmWave cellular systems," *IEEE Trans. Commun.*, vol. 64, no. 9, pp. 3981–3995, Sep. 2016.
[37] J. Arnau, I. Atzeni, and M. Kountouris, "Impact of LOS/NLOS propagation and path loss in ultra-dense cellular networks," in *Proc. IEEE Int. Conf. Commun. (ICC)*, May 2016, pp. 1–6.
[38] I. Atzeni, J. Arnau, and M. Kountouris, "Downlink cellular network analysis with LOS/NLOS propagation and elevated base stations," *IEEE Trans. Wireless Commun.*, vol. 17, no. 1, pp. 142–156, Jan. 2018.
[39] *Study on Channel Model for Frequencies from 0.5 to 100 GHz*, document TR 38.901 V14.0.0, 3rd Generation Partnership Project (3GPP), 2017. [Online]. Available: http://www.3gpp.org/DynaReport/38901.htm
[40] S. Kumar, S. Kalyani, and K. Giridhar, "Spectrum allocation for ICIC-based picocell," *IEEE Trans. Veh. Technol.*, vol. 64, no. 8, pp. 3494–3504, Aug. 2015.
[41] S. Gupta, S. Kumar, R. Zhang, S. Kalyani, K. Giridhar, and L. Hanzo, "Resource allocation for D2D links in the FFR and SFR aided cellular downlink," *IEEE Trans. Commun.*, vol. 64, no. 10, pp. 4434–4448, Oct. 2016.
[42] G. Auer *et al.*, "How much energy is needed to run a wireless network?" *IEEE Wireless Commun.*, vol. 18, no. 5, pp. 40–49, Oct. 2011.
[43] M. Hashemi, C. E. Koksal, and N. B. Shroff, "Energy-efficient power and bandwidth allocation in an integrated sub-6 GHz—Millimeter wave system," 2017, *arXiv:1710.00980*. [Online]. Available: http://arxiv.org/abs/1710.00980
[44] B. Xie, Z. Zhang, R. Q. Hu, G. Wu, and A. Papathanassiou, "Joint spectral efficiency and energy efficiency in FFR-based wireless heterogeneous networks," *IEEE Trans. Veh. Technol.*, vol. 67, no. 9, pp. 8154–8168, Sep. 2018.

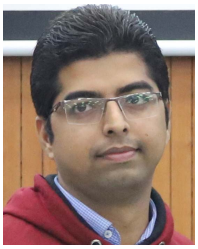

Deepak Saluja received the B.Tech. degree in electronics and communication engineering from Kurukshetra University, India, in 2013, and the M.Tech. degree in wireless communication from Thapar University, Patiala, India, in 2015. He is currently pursuing the Ph.D. degree in electrical engineering with IIT Ropar, India. His research interests include radio resource allocation, RF interference management, vehicular communication, and the IoT networks.

Rohit Singh (Student Member, IEEE) received the B.Tech. degree from the Moradabad Institute of Technology, Moradabad, India, in 2014, and the M.Tech. degree from NIT, Jalandhar, India, in 2017. He is currently pursuing the Ph.D. degree with the Department of Electrical Engineering, IIT Ropar, India. His research interests include self-driving vehicles, vehicular communication, and the IoT connectivity.

Nitin Saluja received the Ph.D. degree in electronics engineering from Thapar University, Patiala, in 2014. He is currently working as an Associate Professor with Chitkara University, Punjab, India. He is specialized in high-frequency engineering including applications in wireless communication including 5G/6G, vehicular communication, industrial microwave driers, and antenna designs. He has won prestigious international awards for microwave and RF engineering applications in food and agriculture applications. He is an inventor of agrionic technologies.

Suman Kumar received the B.Tech. degree in electronics and communication engineering from the Future Institute of Engineering and Management, Kolkata, India, in 2010, and the Ph.D. degree from IIT Madras in 2016. He is currently an Assistant Professor with IIT Ropar. His research interests include performance analysis of wireless networks including RF interference management, HetNets, vehicular communication, and the IoT networks.